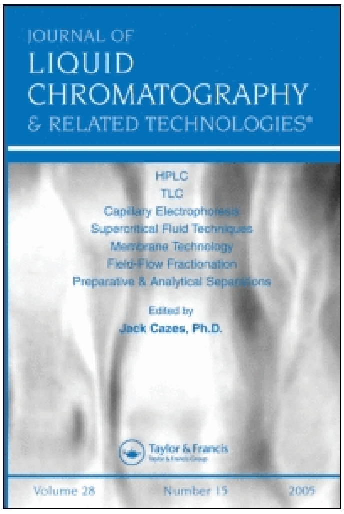

Journal of Liquid Chromatography & Related Technologies
Publication details, including instructions for authors and subscription information:
http://www.informaworld.com/smpp/title~content=t713597273

REVERSED FLOW GAS CHROMATOGRAPHY: A TOOL FOR INSTANTANEOUS MONITORING OF THE CONCENTRATIONS OF REACTANTS AND PRODUCTS IN HETEROGENEOUS CATALYTIC PROCESSES

D. Gavril[a]
[a] Department of Chemistry, University of Patras, Greece

To cite this Article Gavril, D.(2002) 'REVERSED FLOW GAS CHROMATOGRAPHY: A TOOL FOR INSTANTANEOUS MONITORING OF THE CONCENTRATIONS OF REACTANTS AND PRODUCTS IN HETEROGENEOUS CATALYTIC PROCESSES', Journal of Liquid Chromatography & Related Technologies, 25: 13, 2079 — 2099

To link to this Article: DOI: 10.1081/JLC-120013996

URL: http://dx.doi.org/10.1081/JLC-120013996

JOURNAL OF LIQUID CHROMATOGRAPHY & RELATED TECHNOLOGIES
Vol. 25, Nos. 13–15, pp. 2079–2099, 2002

REVERSED FLOW GAS CHROMATOGRAPHY: A TOOL FOR INSTANTANEOUS MONITORING OF THE CONCENTRATIONS OF REACTANTS AND PRODUCTS IN HETEROGENEOUS CATALYTIC PROCESSES

D. Gavril

Department of Chemistry, University of Patras,
26500 Patras, Greece
E-mail: d.gavril@hotmail.com

ABSTRACT

In the present work, the use of an inverse gas chromatographic technique called reversed flow gas chromatography (RFGC) for the study of carbon monoxide oxidation, over different silica supported Pt–Rh alloy catalysts, is reviewed. This technique offers the possibility of the estimation of various physicochemical parameters like overall and time dependent fractional conversions, as well as rate constants, through the instantaneous monitoring of the concentrations of both reactants and products, under steady or non steady-state conditions. These parameters give important information about the activity of the studied catalysts, as well as for the mechanism of the CO catalytic oxidation. The above parameters are in good agreement with the results of other techniques for the same catalysts.

DOI: 10.1081/JLC-120013996
1082-6076 (Print); 1520-572X (Online)

www.dekker.com

Key Words: Inverse gas chromatography; Reversed flow-gas chromatography; Carbon monoxide oxidation; Pt–Rh alloys; Catalysts

INTRODUCTION

Gas chromatography (GC) offers many possibilities for chemical analysis, as well as for physicochemical measurements. Some of the methods, which are used for physicochemical applications, lead to very precise and accurate results with relatively cheap instrumentation and a very simple experimental setup.[1,2] Until a few years ago, such measurements were exclusively based on the traditional techniques of elution development, frontal analysis and displacement development under constant gas flow rate. Studies on diffusion and rate processes were based on the broadening factors, which were embraced by Van Deemter equation.[2] Chapter 12 of reference 2 describes all the above in detail. Another approach to extract physicochemical parameters from elution peaks was based on the analysis of their statistical moments.[3]

Newer physicochemical measurements based on gas chromatography were adsorption studies relating to the determination of adsorption isotherms and other thermodynamic adsorption parameters.[4] The symmetry of chromatographic elution peaks gives qualitative information about the shape of the adsorption isotherm. These peaks are symmetrical only when the isotherm is linear, whereas a convex or a concave isotherm produces peak asymmetry, either in the back or in the front of the peak profile, respectively. Guiochon and his co-workers have made advances on the determination of gas-solid adsorption isotherms, by the so-called step and pulse method.[5,6] Also, Jaulmes et al.[7,8] made a thorough study of peak profiles in non linear gas chromatography, proposing a theoretical model for the profile of elution peaks.

Some of the physicochemical properties measured by GC pertain to solutes dissolved in the mobile carrier-gas phase, but the majority of these properties refer to the stationary phase (e.g., catalytic properties of solid stationary phase for reaction between gases). This is known as *inverse gas chromatography* and has the stationary phase of the system as the main object of investigation. Usually, the same procedures as in direct GC are employed, but the quantities measured (e.g. retention times) are used to derive properties of the stationary phase.

Such an inverse gas chromatographic method is the Reversed Flow Gas Chromatographic (RFGC) technique. In this technique, instead of basing physicochemical measurements on retention volumes of elution peaks, their broadening and their shape distortion, due to physicochemical processes is under study. One can perform such measurements easily and accurately if the chromatographic column, being at a steady-state situation, is perturbed so that it deviates from equilibrium for a short time interval and then is left to return to the original state. This is analogous to relaxation techniques. The perturbation chosen is the change in the direction of flow of the carrier gas, and using a four- or six-port valve connected as shown in Fig. 1 does it. The carrier gas performs only the sampling procedure to measure the gas phase concentration of an analyte at a certain position as function of time. RFGC has been reviewed in 1984,[9] 1988,[10] 1992,[11] and partly in 1995,[12] 1998,[13] and 2000.[14]

It has been used to determine gas diffusion coefficients in binary and ternary mixtures,[15,16] Lenard-Jones parameters,[17] mass transfer coefficients on solids and liquids,[18–22] activity coefficients and solution thermodynamics,[23] adsorption equilibrium constants,[24] solubility and interaction parameters in polymer-solvent systems,[25] time distribution of adsorption energies, local monolayer capacities, local isotherms, and probability density functions for the adsorption energies on heterogeneous surfaces.[26,27]

In the present work, the oxidation of carbon monoxide (CO) over Pt–Rh alloy catalysts was investigated, with the aid of RFGC. The oxidation of CO on noble metals is one of those reactions that can be used to define the field of heterogeneous catalysis. It was one of those reactions used by Berzelius to invent the word "catalysis". This reaction was chosen because of the well-known academic interest in this, as well for its practical importance for the control of hazard emissions. Most of the catalysts used for the control of automotive

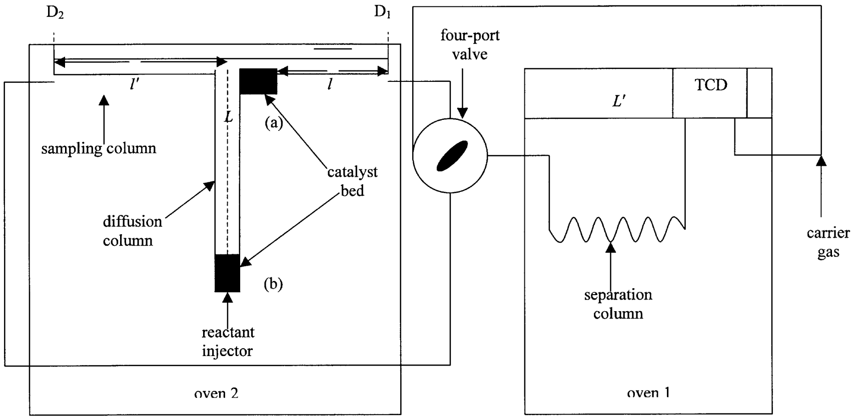

Figure 1. Experimental setup for the kinetic study of carbon monoxide oxidation, over Pt–Rh alloy catalysts: (a) under steady-state conditions, with catalyst bed being put at a short length of column l, near the junction of diffusion and sampling column; (b) under non steady-state conditions, with catalytic bed being put at the top of diffusion column L.

emissions contain platinum or palladium to catalyze the oxidation of carbon monoxide and hydrocarbons to carbon dioxide, as well as rhodium to promote the reduction of nitric oxides. Supported bimetallic catalysts often exhibit certain desirable properties (e.g., improved activity and selectivity, thermal stability, poison resistance, etc.), which are absent in the individual metals. Typical commercial three-way catalysts, used for the simultaneous conversion of carbon monoxide, hydrocarbons, and nitrogen oxides, contain both platinum and rhodium.[28–31] The nature and extent of Pt–Rh interactions in the bimetallic catalysts were ascertained by comparing their catalytic properties with those of pure Pt (active metal for the oxidation of CO and C_xH_y), while holding the absolute amount of each of the noble metals constant.

EXPERIMENTAL

General

The experimental setup for the application of the RFGC technique is very simple and comprises of:

- A conventional gas chromatograph with a thermal conductivity detector (TCD) for the reactant CO and the product CO_2 (oven 1 of Fig. 1) where the separation column L' is incorporated filled with the chromatographic material.
- The sampling column $l'+l$ and the diffusion column L, which was connected perpendicularly to it, to the middle point, were incorporated into oven 2 of Fig. 1. The sampling and the diffusion column form what we call the "*sampling cell*". Both columns were from stainless steel and empty of any material, except for a short length (1 cm) of l near the junction with L (Fig. 1a) or a short length (1 cm) at the top of L (Fig. 1b), where the catalyst bed was contained and heated in the same temperature.
- Sampling cell ends D_1 and D_2 were connected to the carrier gas inlet and the detector through a four-port valve, as shown in Fig. 1, in such a way that the carrier gas flow, through the sampling column (no carrier gas flows through the diffusion column) can be reversed in direction at any time desired and then restored to its original direction. After some time from the introduction of the reactant(s), reversals of the flow direction were started with a very short time elapsing between two successive reversals. Following these flow perturbations, negative and positive abrupt fronts appeared in the chromatogram, forming the so-

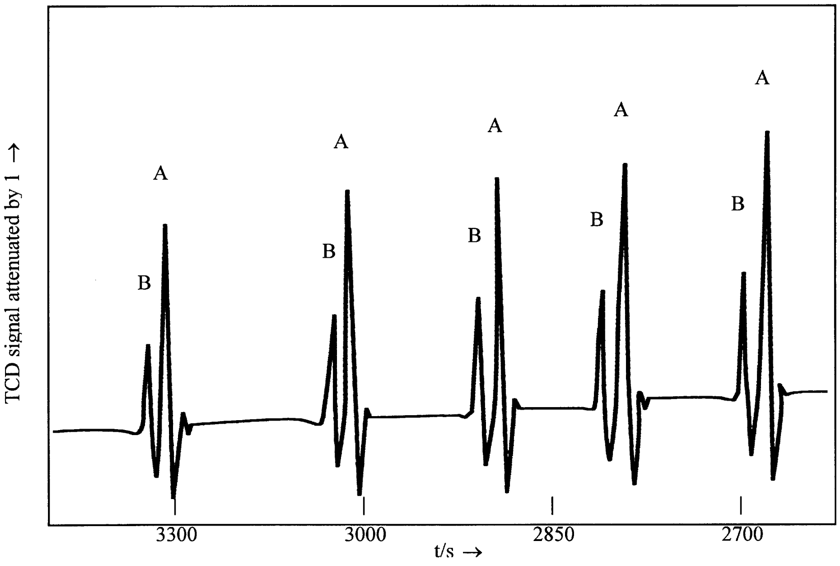

Figure 2. Reversed-flow gas chromatogram showing couples of sample peaks, for the reactant CO (Peak A) and the product CO_2 (Peak B) for experiment done under steady-state conditions, ($T = 340°C$) in the presence of the catalyst 75% Pt + 25% Rh.

called "*sampling peaks*" (Fig. 2). This type of elution curve is predicted by a general chromatographic sampling equation already derived.[9,10]

The height h of the sample peaks measures the concentration of reactant (CO) and product (CO_2), at $x = l'$ and at time t from the beginning of the experiment. If $\ln h$ is plotted against time t for each substance, a so called "*diffusion band*", like those of Fig. 3, is obtained. Using the appropriate mathematical analysis, various parameters like rate constants, activation energies, and fractional conversions can be determined. The reactant oxygen was used in great excess over the other reactant (CO) as a carrier gas mixture (93% v/v He + 7% v/v O_2), while carbon monoxide was not retained on the catalytic bed for a long time, but it was eluted with the produced carbon dioxide.

The use of such an arrangement offers the following advantages, in comparison with other traditional techniques widely used in heterogeneous catalysis:

- It is a very simple arrangement; instead of using flow meters, mixing chambers, saturators, and similar devices to introduce the reaction mixture into the catalyst bed, the reactant is introduced at the top of the

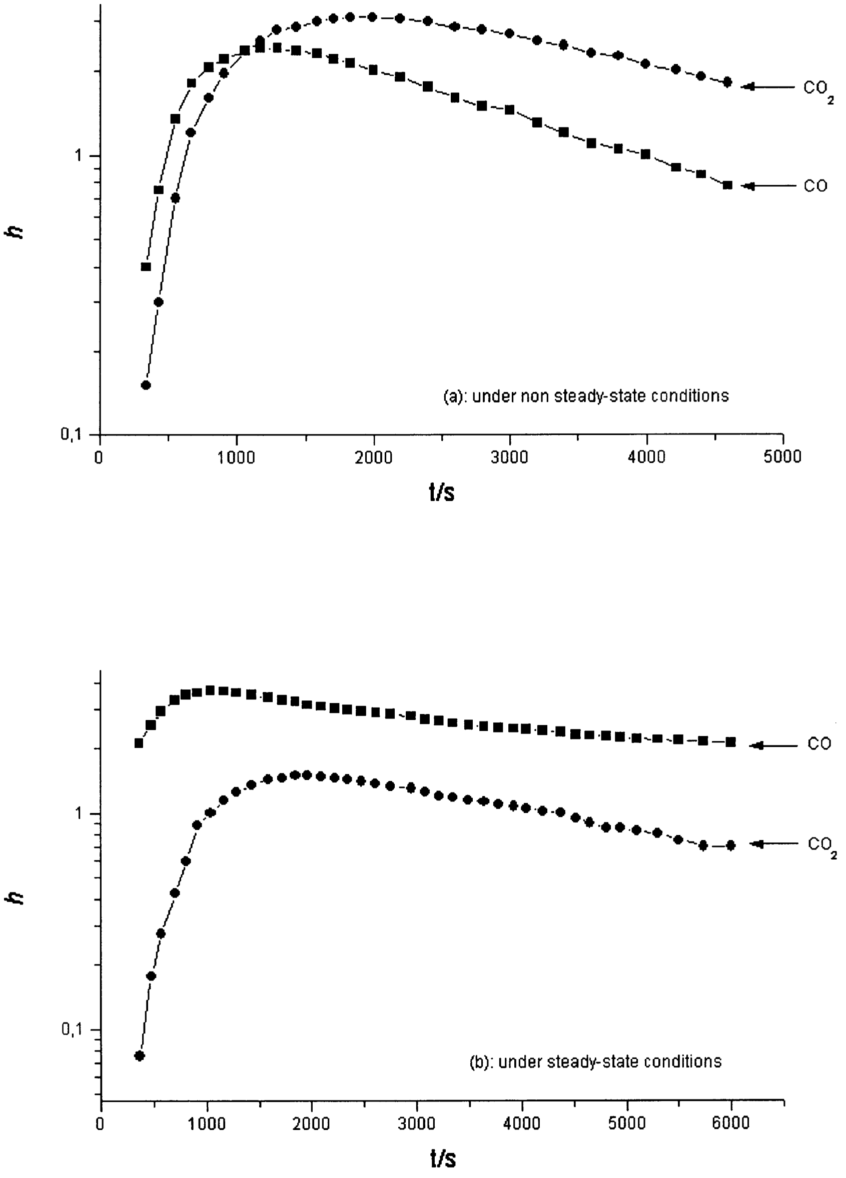

Figure 3. "*Diffusion Bands*" (*h* vs. *t*, in a semi logarithmic scale), of the reactant CO and the product CO_2: (a) for experiment done under non steady-state conditions, at $T = 325°C$, over 100% Pt catalyst and (b) for experiment done under steady-state conditions, at $T = 370°C$, over 25% Pt + 75% Rh catalyst.

diffusion column L by injecting a small volume as a pulse. Then the reactant CO is allowed to diffuse slowly onto the catalyst retained within a short section near the junction of columns L and $l' + l$; each flow reversal is sampling the fractional conversion of reactant to product under steady-state conditions (Fig. 1a). In the experiments that the catalyst is placed at the top of column L (Fig. 1b), a mixture of the reactant CO and product CO_2 is diffused into column L and each flow reversal is sampling the fractional conversion under non steady-state conditions.

- Having placed the catalyst in column l (Fig. 1a), the diffusion feed ensures the presence of reactants over the catalyst bed for a long time period, resembling that of a continuous flow, with a time changing reactant concentration, according to diffusion laws.
- The catalytic bed can be treated either as a differential reactor or an intergraded mode.
- Reversing the flow of the carrier gas causes a sampling of all substances present at $x = l'$. The chromatographic material filling column L', separates these substances, revealing their relative concentrations after passing through the catalyst bed in the form of extra peaks, as shown in Fig. 2. From these sample peaks, the fractional conversions of reactant(s) to product(s) can be calculated many times during a single diffusion feed. Furthermore, the rate constants and the orders of the reactions can be found for an extended range of partial pressures.
- The method, in which the catalytic material is placed in column l (Fig. 1a), works as a pulse technique under steady-state conditions. Thus, it has all the advantages of both a pulse technique and a continuous feeding of the reactant(s). On the other hand, having the catalyst placed at the top of the diffusion column L (Fig. 1b), the method works as a pulse technique under non steady-state conditions. This should lead to kinetic information not masked by adsorption effects of reactant(s) and product(s) on the catalyst surface.

Instrumentation

The stainless-steel separation column L', 45 cm length, filled with silica gel, was incorporated in a commercial gas chromatograph, Shimadzu GC-8A (oven 1 of Fig. 1), equipped with a TC detector.

The stainless-steel "*sampling cell*" was incorporated into a second gas chromatograph, Pye Unicam, Series 104, (oven 2 of Fig. 1). The lengths l' and l of the sampling column were 38 cm each (4 mm ID), while the length L of the diffusion column was 117.6 cm (4 mm ID). The catalytic bed (0.09–018 g) was put either in a short length (1.0 cm) of column *l*, for experiments under steady-state conditions (Fig. 1a), or in the same length at the top of diffusion column *L*, for experiments under non steady-state conditions (Fig. 1b).

Materials

The catalysts studied, which were supplied from Dr. Nieuwenhuys of Laiden University (The Nederlands), were pure Pt, as well as 75% Pt + 25% Rh and 25% Pt + 75% Rh alloys, all supported on SiO_2 (3% w/w). The method of preparation and the surface characterization of the catalysts using TDS and XPS, have been presented previously.[28,29]

Hydrogen, from Linde A. G. (99.999% pure) was used for the reduction of the catalysts. A mixture of 93% v/v helium (99.999% pure) and 7% oxygen (99.999% pure), from B.O.C. Gases was used as carrier gas.

Carbon monoxide from Linde A. G. (99.97% pure) was used as reactant, while the product (CO_2) was identified using carbon dioxide from Matheson Gas Products (99.97% pure).

Procedure

Before any use, the catalysts were reduced at 628K for 10 h in flowing hydrogen, at a flow rate of $1.0\,cm^3\,s^{-1}$. After, the whole system was conditioned by heating, in situ, the catalyst bed at 743K and the chromatographic material at the separation column at 423K, both for 20 h, under carrier gas flowing. Some preliminary injections of the reactant carbon monoxide were made to stabilize the catalytic behavior. Then, $1.0\,cm^3$ of CO, under atmospheric pressure was rapidly introduced, with a gas-tight syringe, at the top of the diffusion column *L*, with the carrier gas flowing in direction from D_1 to D_2 (Fig. 1). After a time of 5 min, a continuous concentration-time curve, owing to both reactant (CO) and product (CO_2), was established and recorded. As it was pointed out before (in General section), during this period, flow reversals of carrier gas direction for 5 s were made, and then the gas was again turned to its original direction, simply by switching the four-port valve from one position to the other and vice-versa. This time period was shorter than the gas hold-up time in column sections l', l and L'. When the gas flow was restored to its original direction, two sample peaks were recorded, like those of Fig. 2. The first belongs to reactant CO and the second to the product CO_2. Repeating the above reversal procedure many times at each temperature, two series of sample peaks were recorded; each pair of them was corresponding to a different time from reactant injection. This means, that using this sampling procedure, we can "watch" and study the catalytic activity at the catalysts steady or non-steady-state condition.

The working temperature range was 553–748K, for the catalyst (oven 2 of Fig. 1), while for the chromatographic material (oven 1 of Fig. 1) it was kept constant at 358K. The variation in the temperature along the catalytic bed, was measured by a digital thermometer Fluke 2190A and was smaller than 1K. The volumetric carrier gas flow rate at ambient temperature was 1.0 $\mathrm{cm^3\,s^{-1}}$. The pressure drop along the whole system was 0.40 atm under steady-state conditions and 0.33 atm under non steady-state conditions.

RESULTS AND DISCUSSION

Two different kinds of fractional conversions were calculated from the heights h of CO and CO_2 sample peaks, which were produced after each flow reversal.

Time dependent fractional conversions, X_t were calculated in every kinetic run, from the following relationship:

$$X_t = \frac{\mathrm{RMR}\ h_{\mathrm{co_2}}}{\mathrm{RMR}\ h_{\mathrm{co_2}} + h_{\mathrm{co}}} \tag{1}$$

where $\mathrm{RMR} = 0.966$ is the relative molar response of the thermal conductivity detector for CO_2 to CO, under the experimental conditions. The heights of the sample peaks were used in the above equation, instead of their areas, because the two sample peaks have approximately the same widths at their half heights.

Overall conversions, X, of carbon monoxide to carbon dioxide, over the studied Pt–Rh alloy catalysts, were calculated from the areas of CO and CO_2 "*diffusion bands*", by using the following equation:

$$X = \frac{\mathrm{RMR\ Area_{co_2}}}{\mathrm{RMR\ Area_{co_2}} + \mathrm{Area_{co}}} \tag{2}$$

As referred in the experimental section a "*diffusion band*" for each substance is obtained, if $\ln h$ is plotted against the time of each flow reversal from the beginning of the experiment t. The area of the "*diffusion band*" (Fig. 3) can easily be estimated from single PC-programmes, like Tblcurve or Origin.

Under Non Steady-State Conditions

Overall percent conversions, $\%X$, of carbon monoxide to carbon dioxide, over the studied Pt–Rh alloy catalysts, under non steady-state conditions (having placed the catalyst at the upper end of the diffusion column L, as shown in Fig. 1b), as function of temperature, are compiled in Table 1.

Temperature variation of these conversions, indicates a characteristic temperature, $T_{\max}$, depending on the catalyst nature, in which maximum overall conversion, $\%X_{\max}$, is achieved. It is obvious, from $\%X_{\max}$ and $T_{\max}$ values, that the two bimetallic catalysts indicate higher catalytic activity than pure Pt, for the CO oxidation reaction. Furthermore, Pt-rich (75% Pt + 25% Rh) catalyst is the more active. Similar results, as far as catalytic activity and temperature variation of conversions, has also been reported for Pt–Rh alloy catalysts, using different experimental techniques.[28,29]

Time dependent fractional conversions, X_t, of CO to CO_2, under non steady-state conditions, at the temperature of maximum overall conversion, for

Table 1. Overall Catalytic Conversions, $\%X$, of CO to CO_2, Over Pt–Rh Alloy Catalysts, in the Presence of Oxygen Excess, Under Non Steady-State Conditions, at Different Temperatures, as Well as Maximum Conversion Values, $\%X_{\max}$, and the Corresponding Temperatures of Maximum Conversion, $T_{\max}$, Determined by RFGC Technique

Catalyst	$T/°C$	$\%X$	$T_{\max}$	$\%X_{\max}$
25% Pt + 75% Rh	325	73.3	390	79.5
	350	74.6		
	375	77.5		
	390	79.5		
	400	77.2		
	425	77.0		
	450	76.8		
75% Pt + 25% Rh	280	82.8	340	87.0
	300	84.8		
	320	85.1		
	340	87.0		
	360	86.0		
	381	84.8		
	401	84.4		
100% Pt	291	50.6	425	67.0
	325	58.7		
	350	60.6		
	375	54.4		
	400	55.1		
	425	67.0		
	458	65.9		

the studied catalysts, are presented in Fig. 4. The maximum time dependent fractional conversions, $\%X_t^{\max}$, are easily estimated from the graphs of this figure and summarized with the corresponding temperatures of maximum overall conversion, $T_{\max}$, for every catalyst, in Table 2.

From the results included in Table 2, as well as from the variation of $\%X_{\max}$ and $\%X_t^{\max}$ with catalyst Pt content shown in Fig. 5, the following conclusions can be extracted:

The $T_{\max}$, $\%X_{\max}$ as well as $X_t^{\max}$ values vary with the catalyst nature, represented from the catalytic Pt content, as follows:

$T_{\max}$ (75% Pt + 25% Rh) < $T_{\max}$ (25% Pt + 75% Rh) < $T_{\max}$ (100% Pt)

$\%X_{\max}$ (100% Pt) < $\%X_{\max}$ (25% Pt + 75% Rh) < $\%X_{\max}$ (75% Pt + 25% Rh)

$\%X_t^{\max}$ (100% Pt) < $\%X_t^{\max}$ (25% Pt + 75% Rh) < $\%X_t^{\max}$ (75% Pt + 25% Rh)

Pt–Rh bimetallic catalysts are more active than pure Pt one. The latter, which has been observed previously[30,31] suggests that there is a synergism between Pt and Rh in the Pt–Rh particles.

From the graphs of time dependent conversions, X_t, of Fig. 4, the following conclusions are drawn:

- All of these graphs have approximately the same shape. They begin from minimum conversion values and end to maximum, $X_t^{\max}$ ones. Especially for the bimetallic catalysts, $X_t^{\max}$ values are almost identical to the overall values, $X_{\max}$, which are estimated from the same experimental data with a different mathematical analysis (from the areas of CO and CO_2 "*diffusion bands*"). The latter is a good indication of the consistency of RFGC technique.
- The kinetic runs of the two more active catalysts (75% Pt + 25% Rh and 25% Pt + 75% Rh) seem to be shorter in duration because of the more rapid consumption of CO, in comparison with those of pure Pt catalyst.
- The rougher change of the shape (slope) in the graphs of the more active bimetallic catalysts, in comparison with the less active of pure Pt, indicates a difference of the corresponding rate constants, which are related with CO oxidation process, over the studied catalytic surfaces. Indeed, such kinetic parameters as rate constants for the carbon monoxide adsorption, desorption and oxidation reaction, as well as the corresponding activation energies have been estimated by RFGC,[32] published, and are in very good agreement with the results of other techniques, giving valuable information for the mechanism of the oxidation reaction over different Pt–Rh alloy catalysts, under non

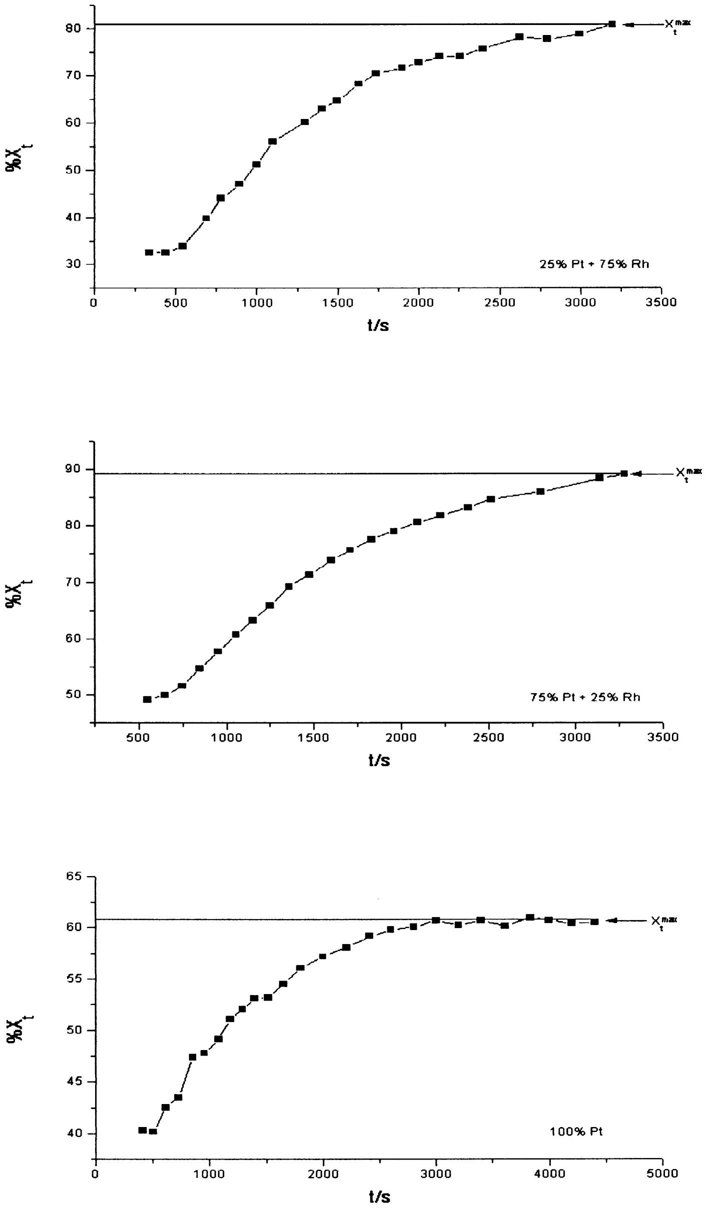

Figure 4. % Time dependent fractional conversions, $\%X_t$, of CO to CO_2, under non steady-state conditions, at the temperature of maximum overall conversion, T_{max}, for the studied Pt–Rh catalysts.

Table 2. Overall Fractional Maximum Conversions, $\%X_{\max}$, and Time Dependent Maximum Fractional Conversions, $\%X_t^{\max}$, of CO to CO_2, Over Pt–Rh Catalytic Alloys, at the Temperatures of Maximum Overall Conversion, $T_{\max}$, Under Non Steady-State Conditions

Catalyst	$T_{\max}/°C$	$\%X_{\max}$	$\%X_t^{\max}$
25% Pt + 75% Rh	390	79.5	81.0
75% Pt + 25% Rh	340	87.0	89.0
100% Pt	425	67.0	62.0

steady-state conditions. In order to have a more assiduous picture of the mechanism of CO catalytic oxidation, rate constants and activation energies were also estimated by RFGC, for the adsorption of CO, O_2 and CO_2, over the above catalysts, under non steady-state conditions.[33,34]

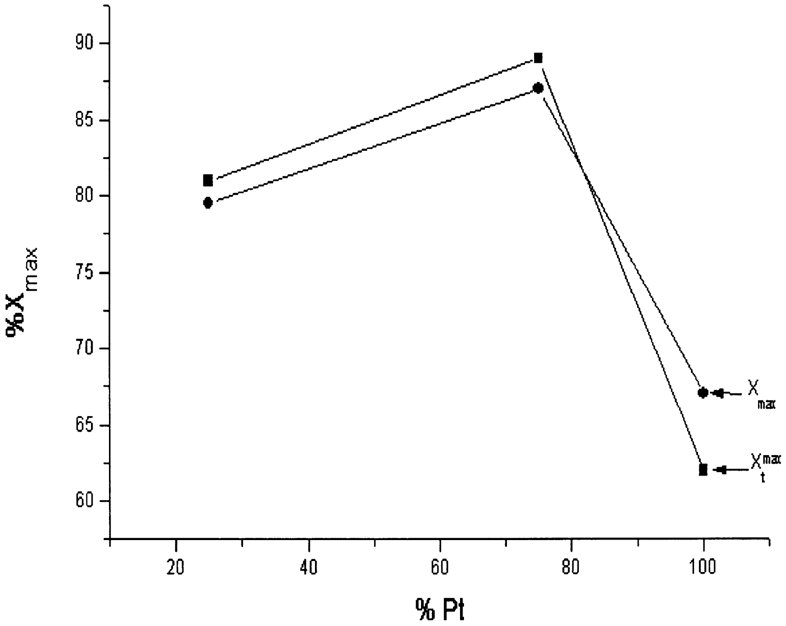

Figure 5. Variation of % maximum overall fractional conversions, $\%X_{\max}$, (●) and % time dependent maximum conversion, $X_t^{\max}$, (■), for the oxidation reaction of carbon monoxide, under non steady-state conditions, over the supported on SiO_2 studied catalysts, with the atomic percentage of catalyst Pt.

Under Steady-State Conditions

The following observations can be drawn from the comparison of the indicating "*diffusion bands*" under non-steady and steady state conditions, shown in Fig. 3:

- In both cases, CO_2 diffusion bands have a similar shape, increase roughly until a maximum, and then slowly decrease.
- However, there is a visible difference in the shapes of carbon monoxide bands due to the different feeding of the catalytic bed with carbon monoxide. Under steady-state conditions, there is a continuous feeding of the catalyst with smaller quantities of diffusing CO, but the corresponding fractional conversions are smaller, as it is concluded from the higher h values. A possible explanation is the shorter time during which the reactants stay on the catalytic surface, due to the continuous carrier gas flow, compared to that under non steady-state conditions.

Overall percent conversions, $\%X$, of CO to CO_2 and their temperature variation under steady-state conditions, having the catalyst placed in a short length of column l (Fig. 1a) over the bimetallic catalysts used, are presented in Fig. 6.

The observations listed below can be drawn from the results shown in Fig. 6:

- The percent maximum overall fractional conversion, $\%X_{\max}$, for the catalyst of bigger conversion (75% Pt + 25% Rh), is approximately equal to the average value of individual overall conversions and independent of temperature, in the working temperature range (281–425°C).
- The overall fractional conversion values, $\%X$, for the rest of the two catalysts (100% Pt, 25% Pt + 75% Rh), increase with temperature until a constant maximum value, $\%X_{\max}$, is obtained.
- The maximum overall conversion values, $\%X_{\max}$, vary with Pt content in the catalytic alloy, as follows:
- $\%X_{\max}$ (25% Pt + 75% Rh) < $\%X_{\max}$ (100% Pt) < $\%X_{\max}$ (75% Pt + 25% Rh)
- The temperature, $T_{\max}$, at which maximum constant, $\%X_{\max}$, is obtained for every studied catalyst, varies in the following order:
- $T_{\max}$ (75% Pt + 25% Rh) < $T_{\max}$ (100% Pt) < $T_{\max}$ (25% Pt + 75% Rh)

It is concluded from the above observations, that the most active catalyst is Pt-rich and follows Pt-pure and finally Rh-rich. The Pt-rich catalyst is also the more active under non steady-state conditions. But, it is contrary to that found

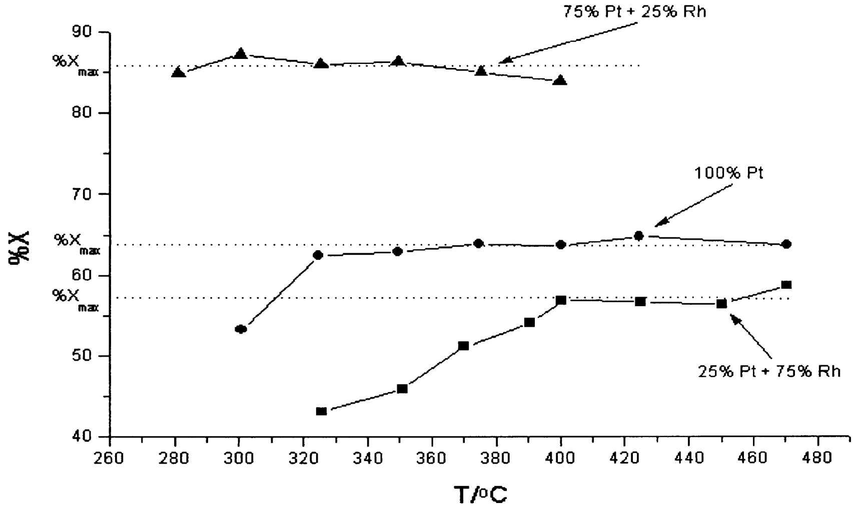

Figure 6. Temperature variation of % overall fractional conversions, %X, for the catalytic oxidation of CO to CO_2, under steady-state conditions.

under non steady-state conditions, that the Rh-rich catalyst is more active than the Pt-pure one. In accordance with that result of higher CO to CO_2 conversion over Pt-pure catalyst than Rh-rich one, the values of the rate constants, k, which are calculated by Eq. (3)[35] and the temperature variation of them, are presented in Fig. 7:

$$k = \frac{V}{w} \ln \frac{1}{(1 - X)} \tag{3}$$

where: k is the rate constant ($m^3\,kg_{catalyst}{}^{-1}\,s^{-1}$) for the catalytic oxidation reaction of CO to CO_2, V is the volumetric flow rate ($m^3 s^{-1}$) of the reacting mixture (carrier gas: $He + O_2$ and CO) corrected at the catalyst temperature and pressure and X the overall fractional conversion (estimated by the areas of CO and CO_2 "*diffusion bands*").

The rate constant k values are generally higher for the Pt-rich catalyst. The k values of Pt-rich catalyst are also higher than those of Rh-rich one. This behavior can be attributed to the fact, that during continuous feeding of the catalytic bed with oxygen, which is contained in the carrier gas, the Rh-active sites of the catalytic alloy, are covered by oxygen not leaving enough active sites vacant for CO adsorption (as much needed from the stoichiometry of the reaction). Thus, the catalytic fractional conversions and the corresponding rate constants for the carbon monoxide oxidation reaction are decreased, as the

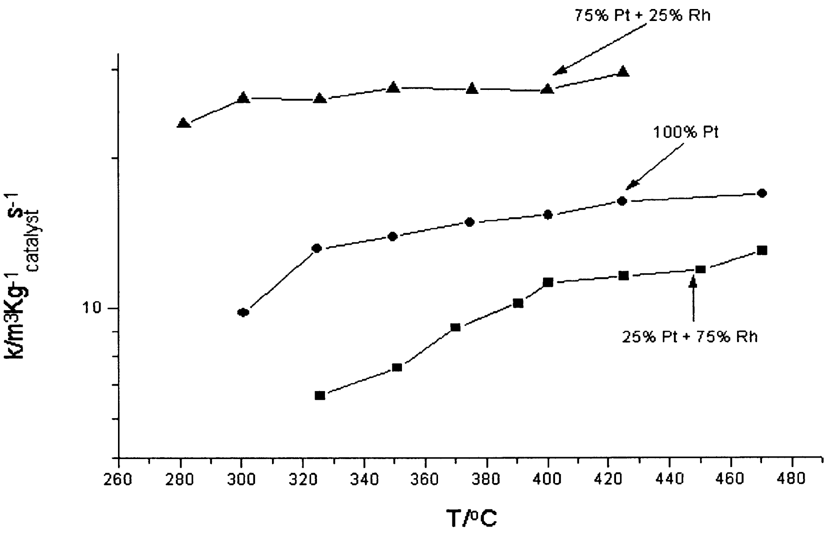

Figure 7. Temperature dependence of the rate constants, $k/m^3\ kg_{catalyst}{}^{-1}\ s^{-1}$, in a semi logarithmic scale, for the reaction of carbon monoxide oxidation, over the studied Pt–Rh alloy catalysts, under steady-state conditions.

probability of CO molecules and O atoms being adsorbed to neighboring sites decreases. The fact that oxygen adsorption is bigger on Rh-sites and, consequently, to Rh-rich catalysts has been also observed previously,[28–31] with other techniques and in oxygen adsorption experiments under non steady-state conditions, by RFGC.[33,34]

Time dependent fractional conversions for the studied catalysts, X_t, of CO to CO_2 under steady-state conditions, at the temperature of maximum overall conversion, are presented in Fig. 8. Maximum time dependent fractional conversions, X_t^{max}, are easily estimated from the graphs of Fig. 8 and summarized with the maximum overall conversions and the corresponding temperatures, for every catalyst in Table 3. From these graphs (of Fig. 8), their comparison with corresponding graphs under non steady-state conditions (Fig. 4), as well as from the results of Tables 2 and 3, the following conclusions can be drawn:

- It is observed, from the shape of the time dependent conversion graphs, of Fig. 4 and 8, that although under non steady-state conditions, the graph ends when a maximum value, X_t^{max} is obtained under steady-state conditions; it continues for a long time interval (~3000 s) during which the maximum X_t^{max}, value is kept constant.

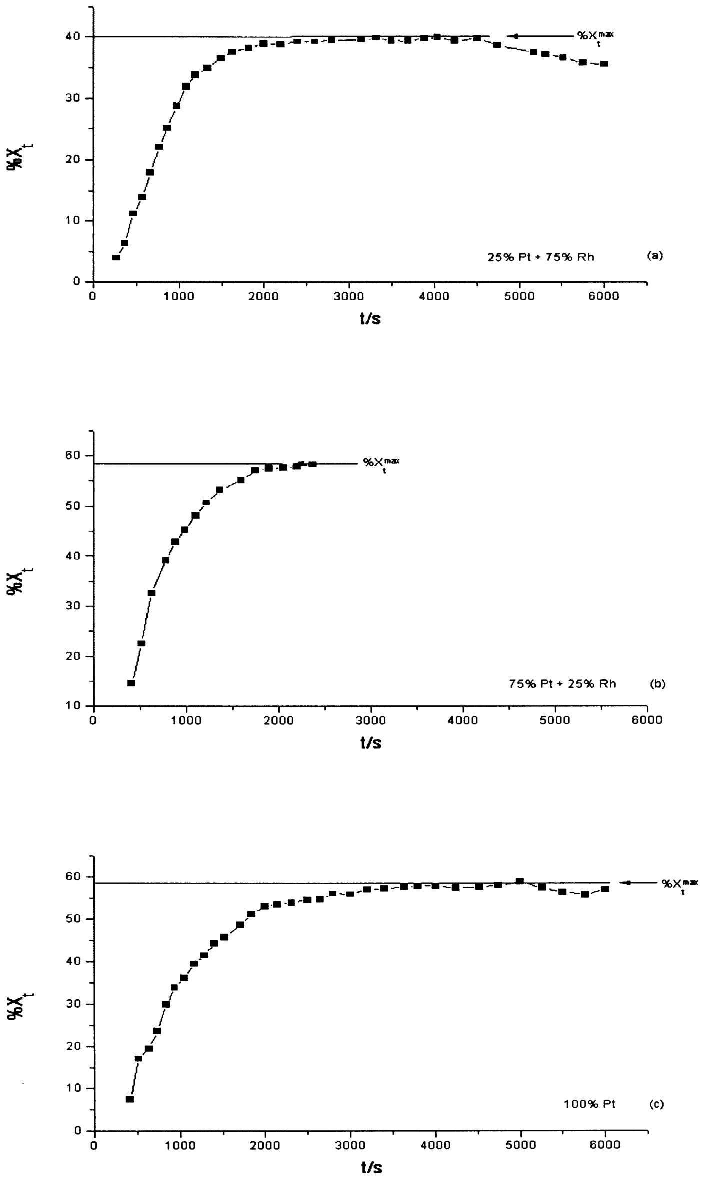

Figure 8. Time variation of % catalytic fractional conversions, of CO to CO_2, $\%X_t$, at the temperature of maximum overall conversion, T_{max}, for experiments done under steady-state conditions, (a) at 401°C, over 25% Pt + 75% Rh, (b) at 350°C, over 75% Pt + 25% Rh, (c) at 325°C, over 100% Pt silica supported catalyst.

Table 3. Overall Fractional Maximum Conversions, $\%X_{\max}$, and Time Dependent Maximum Fractional Conversions, $\%X_t^{\max}$, of CO to CO_2, Over Pt–Rh Catalytic Alloys, at the Temperatures of Maximum Overall Conversion, $T_{\max}$, Under Steady-State Conditions

Catalyst	$T_{\max}/^\circ C$	$\%X_{\max}$	$\%X_t^{\max}$
25% Pt + 75% Rh	>401	57.2	40.0
75% Pt + 25% Rh	>281	85.5	58.0
100% Pt	>325	64.1	58.0

- Furthermore, X_t values finally slightly decrease, for Rh-rich catalyst, because of the probable deactivation of this catalyst.
- The kinetic runs under steady-state conditions, seem to have bigger duration, except of those of the most active 75% Pt + 25% Rh catalyst, due to the faster CO consumption. The reason is the continuous feeding of the catalytic bed, with diffusing CO, in contrast with the experiments under non steady-state conditions, where the reactant CO is introduced as a pulse at the catalytic bed.
- The overall fractional conversions values, for the Rh-rich catalyst under steady-state conditions, are much smaller in comparison with those under non steady-state conditions. It can be attributed to the fact that continuously flowing oxygen (of the carrier gas) covers Rh-active sites, not leaving enough active sites vacant for CO adsorption, as well as to the smaller contact time of the reactants on the active surface. The X values for the Pt-rich catalyst are also slightly smaller due to the smaller time of contact of the reactants on the catalytic surface, while the same values for the Pt-pure catalyst are generally higher than those under non steady-state conditions.
- An interesting difference observed under steady-state conditions, is the deviation between the maximum conversions, $X_{\max}$ and the maximum time dependent conversions, $X_t^{\max}$. These values are almost identical under non steady-state conditions, while the $X_t^{\max}$ values are much smaller than the $X_{\max}$ ones, under steady-state conditions, as shown in Tables 2 and 3. The latter can be attributed to the different kind of feeding of the catalytic bed, which results in a much smaller time that the reactants remain on neighboring active sites. The kinetic run practically ends at a maximum conversion value under non steady-state conditions, while under steady-state conditions it continues until a constant maximum conversion for a significant time interval, as explained previously. Thus,

although the $X_t^{\max}$ values are much smaller in comparison with those under non steady-state conditions, the overall conversions (with the exception of Rh-rich catalyst) are not so small.

Finally, from the shape of the temperature variation graphs of the overall conversions, as shown in Fig. 6, interesting conclusions can be drawn for the mechanism of the oxidation under continuous CO feeding of the catalytic bed.

- Carbon monoxide oxidation reaction, at the most active catalyst 75% Pt + 25% Rh, is kinetically controlled.
- While, for the Pt-pure, the internal diffusion of the reactant(s) into pores of the catalyst process, is the rate-determining step.
- And the external diffusion of the reactant(s) from the gas phase to the pores of the catalyst, is the rate-determining step at the less active Rh-rich catalyst.

As a general conclusion, it could be said that reversed flow gas chromatography can be an excellent "tool" for instantaneous monitoring of the concentrations of reactants and products in a heterogeneous catalytic process like the oxidation of carbon monoxide, over Pt-Rh alloy catalysts. Furthermore, this gas chromatographic "tool" offers many other possibilities, not only for the monitoring of the reactants and products, but also for the estimation of various physicochemical parameters through the above monitoring, simply and accurately. Such parameters are: the overall and time dependent fractional conversions under steady or non steady-state conditions for the catalytic oxidation of carbon monoxide,[35] which are referred in the present work, as well as rate constants, activation energies, and surface diffusion coefficients for the catalytic oxidation of CO[32,36] and the adsorption of CO, O_2 and CO_2,[33,34] in these catalysts that have been studied previously.

REFERENCES

1. Laub, R.J.; Pescok, R.L. *Physicochemical Applications of Gas Chromatography*; Wiley: New York, 1978.
2. Conder, J.R.; Young, C.L. *Physicochemical Measurements by Gas Chromatography*; Wiley: Chichester, 1979.
3. Suzuki, M.; Smith, J.M. Transport and Kinetic Parameters by Gas Chromatographic Techniques. Adv. Chromatogr. **1975**, *13*, 213–263.
4. Kiselev, A.V.; Yashin, Y.I. *Gas Adsorption Chromatography*; Plenum Press: New York, 1969.
5. Dondi, F.; Gonnord, M.F.; Guiochon, G. Chromatographic Determination of Gas–Solid Adsorption Isotherms by the Step and Pulse Method I.

Apparatus and Data Processing. J. Colloid Interphase Sci. **1977**, *62*, 303–315.

6. Dondi, F.; Gonnord, M.F.; Guiochon, G. Chromatographic Determination of Gas–Solid Adsorption Isotherms by the Step and Pulse Method. II. Choice of a Model for the Adsorption Isotherm of Benzene and Cyclohexane on Graphitized Carbon Black. J. Colloid Interphase Sci. **1977**, *62*, 316–328.
7. Jaulmes, A.; Vidal-Madjar, C.; Ladurelli, A.; Guiochon, G. Study of Peak Profiles in Nonlinear Gas Chromatography 1. Derivation of a Theoretical Model. J. Phys. Chem. **1984**, *88*, 5379–5385.
8. Jaulmes, A.; Vidal-Madjar, C.; Ladurelli, A.; Guiochon, G. Study of Peak Profiles in Nonlinear Gas Chromatography. 2. Determination of the Curvature of Isotherms at Zero Surface Coverage on Graphitized Carbon Black. J. Phys. Chem. **1984**, *88*, 5385–5391.
9. Katsanos, N.A.; Karaiskakis, G. In *Advances in Chromatography*; Giddings, J.C., Grushka, E., Cazes, J., Brown, P.R., Eds.; Marcel Dekker, New York, 1984; 125–180.
10. Katsanos, N.A. *Flow Perturbation Gas Chromatography*; Marcel Dekker, New York, 1988; 87–296.
11. Katsanos, N.A. In *Theoretical Advancement in Chromatography and Related Separation Techniques*; Dondi, F., Guiochon, G., Eds.; Kluwer Academic Publisher: Amsterdam, 1992; 349–367.
12. Katsanos, N.A.; Roubani-Kalantzopoulou, F. J. Chromatogr. A **1995**, *710*, 191–228.
13. Katsanos, N.A.; Thede, R.; Roubani-Kalantzopoulou, F. J. Chromatogr. A **1998**, *795*, 133–184.
14. Katsanos, N.A.; Roubani-Kalantzopoulou, F. Advances in Physicochemical Measurements Using Inverse-Gas Chromatography. In *Advances in Chromatography*, Brown, P.R., Grushka, E., Eds.; Marcel Dekker: New York, 2000; 231–273.
15. Katsanos, N.A.; Karaiskakis, G. J. Chromatogr. **1982**, *237*, 1–14.
16. Rashid, K.A.; Gavril, D.; Karaiskakis, G. Instr. Sci. Tech., *in press.*
17. Karaiskakis, G. J. Chromatogr. Sci. **1985**, *23*, 360–365.
18. Katsanos, N.A.; Agathonos, P.; Niotis, A. J. Phys. Chem. **1988**, *92*, 1645–1650.
19. Gavril, D.; Karaiskakis, G. Instr. Sci. & Tech. **1997**, *25* (3), 217–234.
20. Gavril, D.; Karaiskakis, G. Chromatographia **1998**, *47* (1/2), 63–71.
21. Gavril, D.; Rashid, K.A.; Karaiskakis, G. J. Chromatogr. A **2001**, *919*, 349–356.
22. Rashid, K.A.; Gavril, D.; Katsanos, N.A.; Karaiskakis, G. J. Chromatogr. A **2001**, *934*, 31–49.
23. Katsanos, N.A.; Karaiskakis, G.; Agathonos, P. J. Chromatogr. **1986**, *349*, 369–380.

24. Karaiskakis, G.; Katsanos, N.A.; Niotis, A. J. Chromatogr. **1982**, *245*, 21–26.
25. Agathonos, P.; Karaiskakis, G. J. Appl. Polymer. Sci. **1989**, *37*, 2237–2243.
26. Katsanos, N.A.; Arvanitopoulou, E.; Roubani-Kalantzopoulou, F.; Kalantzopoulos, A. J. Phys. Chem. B **1999**, *103*, 1152–1157.
27. Katsanos, N.A.; Iliopoulou, E.; Roubani-Kalantzopoulou, F.; Kalogirou, E. J. Phys. Chem. B **1999**, *103*, 10228–10233.
28. Wolf, R.M.; Siera, J.; van Delft, F.C.M.J.M.; Nieuwenhuys, B.E. Faraday Discuss. Chem. Soc. **1989**, *87*, 275–280.
29. van Delft, F.C.M.J.M.; Nieuwenhuys, B.E.; Siera, J.; Wolf, R.M. ISIJ Int. **1989**, *29*, 550–558.
30. Oh, S.H.; Carpenter, J.E. J. Catal. **1986**, *98*, 178–190.
31. Hu, Z.; Allen, F.M.; Wan, C.Z.; Heck, R.M.; Steger, J.J.; Lakis, R.E.; Lyman, C.E. J. Catal. **1998**, *174*, 13–21.
32. Gavril, D.; Katsanos, N.A.; Karaiskakis, G. J. Chromatogr. A **1999**, *852*, 507–523.
33. Gavril, D.; Karaiskakis, G. J. Chromatogr. A **1999**, *845*, 67–83.
34. Gavril, D.; Koliadima, A.; Karaiskakis, G. Langmuir **1999**, *15*, 3798–3806.
35. Gavril, D.; Koliadima, A.; Karaiskakis, G. Chromatographia **1999**, *49* (5/6), 285–292.
36. Katsanos, N.A.; Gavril, D.; Karaiskakis, G. J. Chromatogr. A, *in press*.

Received February 14, 2002
Accepted March 30, 2002
Manuscript 5774